Type I Collagen-Functionalized Supported Lipid Bilayer as a Cell Culture Platform

Chun-Jen Huang,[†,‡] Nam-Joon Cho,[†,§,||] Chih-Jung Hsu,[†,‡,⊥] Po-Yuan Tseng,[‡] Curtis W. Frank,[*,§] and Ying-Chih Chang[*,‡]

Genomics Research Center, Academia Sinica, Taipei 115, Taiwan, and Department of Chemical Engineering, Stanford University, Stanford, California 94305

Received December 20, 2009; Revised Manuscript Received February 10, 2010

The supported phospholipid bilayer serves as an important biomimetic model for the cell membrane in both basic and applied scientific research. We have constructed a biomimetic platform based on a supported phospholipid bilayer that is functionalized with type I collagen to serve as a substrate for cell culture. To create the type I collagen-functionalized lipid bilayer assembly, a simple chemical approach was employed: lipid vesicles composed of 1-palmitoyl-2-oleoyl-*sn*-glycero-3-phosphocholine (POPC) and 1,2-dipalmitoyl-*sn*-glycero-3-phosphoethanolamine-*N*-(glutaryl) (DP-NGPE), a carboxylic acid-functionalized phospholipid, were prepared and then fused onto an SiO_2 substrate to form a supported lipid bilayer. Subsequently, type I collagen molecules were introduced to form stable collagen−lipid conjugates via amide linkages with activated DP-NGPE lipids. The binding kinetics of the conjugation process and the resultant changes in film thickness and viscoelasticity were followed using the quartz crystal microbalance with dissipation (QCM-D) monitoring. The morphology of the conjugated collagen adlayer was investigated with atomic force microscopy (AFM). We observed that the adsorbed collagen molecules tended to self-assemble into fibrillar structures. Fluorescence recovery after photobleaching (FRAP) was utilized to estimate lateral lipid mobility, which was reduced by up to 20% after the coupling of type I collagen to the underlying lipid bilayer. As a cell culture platform, the collagen-conjugated supported lipid bilayer showed promising results. Smooth muscle cells (A10) retained normal growth behavior on the collagen-functionalized platform, unlike the bare POPC lipid bilayer and the POPC/DG-NGPE bilayer without collagen. The biomimetic functionalized lipid system presented here is a simple, yet effective approach for constructing a cell culture platform to explore the interactions between extracellular matrix components and cells.

Introduction

The cell membrane is a highly organized structure that mediates cellular activities in response to specific and nonspecific extracellular signals and that maintains the critical concentration gradients between the cytosol and extracellular spaces.[1–3] These extracellular signals, transmitted by membrane receptors and integrated by intracellular pathways, regulate gene expression and control the behavior of individual cells.[1–3] Cell biology and tissue engineering research has been rapidly advanced by greater understanding of cell and extracellular matrix (ECM) interfaces,[4–6] which have led to the design of new biomimetic platforms.[7–9]

Type I collagen is the most abundant ECM protein, consisting of triple helical collagen molecules.[10] The fibrillogenesis of type I collagen occurs via self-assembly that is guided by interactions between collagen molecules, followed by organization of the fibrils into fibers capable of supporting different types of tensile stresses.[11,12] Amino acid domains of type I collagen selectively regulate the binding of cell membrane receptors and promote cell adhesion, proliferation, and differentiation. These characteristics have been utilized to manipulate cell culture microenvironments[4,13,14] and to study the molecular dynamics and binding mechanisms of particular integrin receptors.[15]

An examination of the dynamics and structure of ECM proteins in artificial cell membranes would extend our knowledge of the recognition mechanisms between matrix proteins and their specific membrane receptors and would further our understanding of the interfaces between lipid molecules and complex biomacromolecules. A supported lipid bilayer functionalized with biospecific ligands is valuable for studying cell−macromolecule interactions and cell−cell interactions.[16–20] Besides its biological implications, such a functionalized lipid bilayer may also serve as a sensing platform, since it effectively reduces nonspecific binding. Earlier efforts defined peptide-lipid interfaces as simplified versions of complex biological systems.[21–24] For example, chemical modification of a small fraction of amphiphiles with the tripeptide Arg-Gly-Asp (RGD) in Langmuir−Blodgett supported films permitted the manipulation of the cell adhesion pattern.[25–28] RGD is a minimal cell recognition peptide sequence that specifically binds to receptors (e.g., $\alpha_v\beta_3$) on cell surfaces. Beyond ligand−receptor interactions, it is believed that the intrinsic physical properties of ECM proteins play a key role in the regulation of cell behavior.

In this article, we have constructed a particular ECM protein−lipid assembly, specifically a type I collagen-functionalized supported lipid bilayer on an SiO_2 substrate. As compared to past efforts to mimic the ECM by directly conjugating type I collagen molecules to amine-functionalized inorganic substrates,[29,30] the model system presented here considers the interactions between type I collagen

* To whom correspondence should be addressed. E-mail: yingchih@gate.sinica.edu.tw, cwfrank@stanford.edu.
† Contributed equally to this work.
‡ Genomics Research Center.
§ Stanford University.
|| Current Address: Department of Medicine, Division of Gastroenterology and Hepatology, Stanford University School of Medicine, Stanford, CA 94305.
⊥ Current Address: Department of Chemistry, University of Pennsylvania, Philadelphia, PA 19104.

10.1021/bm901445r
Published on Web 04/02/2010

molecules and the underlying bilayer, which better mimics the cellular environment where such lipid−collagen interactions are necessary for many biological activities. Our platform employs simple chemistry to attach type I collagen directly to the bilayer, as inspired by real biological systems where membrane proteins such as integrins serve as the chemical linker. Previously, the ε-amino group side chains of lysine residues on type I collagen have been targeted as sites for chemical modification.[31–34] In the present study, we prepared various compositions of binary lipid mixtures using chemically inert 1-palmitoyl-2-oleoyl-*sn*-glycero-3-phosphocholine (POPC) and 1,2-dipalmitoyl-*sn*-glycero-3-phosphoethanolamine-*N*-(glutaryl) (DP-NGPE), which carries a free carboxylic acid for chemical modification. We were able to control the quantity of adsorbed type I collagen by systematically changing the percentage of functionalized DP-NGPE in the bilayer, thereby modulating its molecular orientation, conformation, and surface coverage.

To investigate the binding kinetics, molecular orientation, and thickness of conjugated type I collagen, as well as the lateral lipid mobility of the underlying model lipid bilayer, we employed three different analytical techniques: quartz crystal microbalance with dissipation (QCM-D) monitoring, atomic force microscopy (AFM), and fluorescence recovery after photobleaching (FRAP). Following platform characterization, we measured the attachment and growth of smooth muscle cells (A10). The collagen-functionalized bilayer platform supported normal cell growth, while two control platforms, a bare lipid bilayer (POPC) and a functionalized lipid bilayer (POPC/DP-NGPE) without collagen, did not support regular cell growth. Thus, the type I collagen-functionalized lipid bilayer offers an improved environment for cell growth. Further, this novel platform can be used to study ligand−cell interactions in an environment that better represents the extracellular interface of the cell membrane.

Materials and Methods

Materials. *N*-(3-Dimethylaminopropyl)-*N*′-ethylcarbodiimide hydrochloride (EDC) and sulfo-*N*-hydroxysuccinimide (sNHS) were purchased from Pierce (Rockford, IL). 1,2-Dipalmitoyl-*sn*-glycero-3-phosphoethanolamine-*N*-(glutaryl) (DP-NGPE), 1-palmitoyl-2-oleoyl-*sn*-glycero-3-phosphocholine (POPC), and the vesicle extrusion accessories were obtained from Avanti Polar Lipids (Alabaster, AL). *N*-(7-Nitrobenz-2-oxa-1,3-diazol-4-yl)-1,2-dihexadecanoyl-*sn*-glycero-3-phosphoethanolamine, triethylammonium salt (Texas Red- DHPE), and type I collagen (rat tail) were purchased from Molecular Probes (Eugene, OR) and BD Bioscience (Franklin Lakes, NJ), respectively. Deionized and filtered water (resistivity > 18.2 MΩ·cm) was used throughout the work (Milli-Q, Millipore, Billerica, MA). For each coupling reaction, we utilized a different buffer: Tris buffer at pH 5.5 for activating the NHS ester-functionalized lipid and Tris buffer at pH 7.2 for conjugation and washing. All buffers were filtered and degassed before use. The Willco-dish (glass bottom dish) for the FRAP experiments was from Leica (Wetzlar, Germany).

Small Unilamellar Vesicle Preparation. Small unilamellar vesicles consisting of POPC mixed with DP-NGPE, whose weight percentage varied from 0 to 40%, were prepared by the extrusion method. For FRAP measurements, a weight ratio of 99.5:0.5 for a single lipid or mixture of lipids with Texas Red-DHPE was prepared. Extruded unilamellar vesicles (referred to simply as vesicles) were prepared in the following manner. Lipid films were prepared by drying the lipids, initially dissolved in chloroform, under a gentle stream of nitrogen gas at room temperature. The resulting lipid film was then placed under vacuum overnight to evaporate any residual chloroform. Multilamellar vesicles were prepared by first swelling the lipid film in aqueous solution, then vortexing periodically for five minutes. EDC (50 μL of a 60 mg/mL solution in pH 5.5 Tris buffer) and sNHS (50 μL of a 60 mg/mL solution in pH 5.5 Tris buffer) were mixed with 200 μL of vesicle solution for 2 h to convert the carboxyl groups of DP-NGPE to chemically active *O*-acylisourea esters (referred to as NHS-ester groups).[35] The resulting multilamellar vesicles were subsequently sized by a mini-extruder (Avanti Polar Lipids) through 100, 50, and 30 nm track-etched polycarbonate membranes, resulting in small unilamellar vesicles. Vesicles were generally prepared at a nominal lipid concentration of 5 mg/mL and then diluted before experiment.

Conjugation of Collagen Molecules with Supported Lipid Bilayer. The collagen solution (0.2 mg/mL) was prepared by diluting the stock 4 mg/mL collagen solution with pH 7.2 Tris buffer. For the QCM-D measurements, 1.0 mL of the temperature-stabilized diluted collagen solution was introduced into the QCM-D chamber containing predeposited supported lipid bilayers. The chamber was then rinsed with pH 7.2 Tris buffer to remove the loosely bound collagen molecules. For the FRAP and TM-AFM measurements, the supported bilayers were incubated in 1.0 mL of the 0.2 mg/mL collagen solution for 1 h. Unbound collagen molecules were washed away with pH 7.2 Tris buffer.

A10 Smooth Muscle Cell Culture. The A10 smooth muscle cell line was purchased from the American Type Culture Collection (Rockville, MD). The cells were maintained in a humidified incubator with 5% CO_2 at 37 °C and grown on 25 cm^2 cell culture flasks (Corning Incorporated, Corning, NY) for regular culture or a WillCo-dish for bilayer experiments in Dulbecco's modified Eagle's medium (DMEM) with high glucose (Invitrogen, Carlsbad, CA), which was supplemented with 10% fetal bovine serum (Hyclone Laboratories, Logan, UT), 2 mM of L-glutamine, 100 units/mL penicillin, and 100 g/mL streptomycin (Invitrogen). A10 cells were treated with 1X 0.25% trypsin (Invitrogen) at 37 °C for 3 min to detach the cells from the culture dish surfaces. Functionalized lipid bilayers containing POPC and 20% DP-NGPE, with and without conjugated collagen, were prepared on hydrophilic glass WillCo-dishes. In each trial, 800000 cells were added to each WillCo-dish containing 2 mL of DMEM. After incubating the cells on the bilayer overnight, the dishes were then rinsed with 1X PBS (Hyclone) three times to remove unbound cells and then observed using a Leica DMIRE2 inverted microscope (Wetzlar, Germany). The statistics of cell adherent area and cell number were calculated with Metamorph software (Molecular Devices, Downingtown, PA).

QCM-D Measurement and Modeling. QCM-D was used to monitor the resonance frequency shift (Δf) and energy dissipation shift (ΔD) caused by deposition of the adlayer on the quartz crystal. The experimental measurements were obtained with a Q-sense D300 instrument (Q-sense AB, Gothenburg, Sweden). The D300 allows simultaneous measurements of Δf and ΔD at multiple overtones (n = 1, 3, ..., i.e., f = 5 MHz, 15 MHz, ...) up to $n = 7$, to obtain the resonant frequencies, $f_{n=1}$, $f_{n=3}$, and so on, and the corresponding dissipation values, $D_{n=1}$, $D_{n=3}$, and so on, with a repetition rate of ∼1 Hz. A small mass (Δm) adsorbed on the quartz sensor induces a decrease in resonance frequency (Δf), which is proportional to Δm:

$$\Delta m_{\text{Sauerbrey}} = -\frac{C_{\text{QCM}}\Delta f}{n} \tag{1}$$

where C_{QCM} is the mass-sensitivity constant (= 17.7 ng cm^{-2} Hz^{-1} at f = 5 MHz), and n is the overtone number (= 1, 3, 5, and 7). Equation 1 is the ideal case only for a rigid adlayer with low energy dissipation. Because the linear relationship between the adsorbed mass and the change in frequency (eq 1) is not necessarily valid for viscoelastic films, which exhibit additional energy dissipations as well as overtone-dependent frequency and dissipation responses, it is necessary to use a modeling approach to understand viscoelastic systems.[36–38]

The Voigt−Voinova model includes these viscoelastic effects and assumes uniform thickness, uniform film density, a Newtonian liquid, and no slip. Further, it is assumed that the film viscosity is independent of overtone frequencies. Then, Δf and ΔD can be related to the film

density, viscoelastic properties, and thickness in terms of a Taylor expansion:[38–40]

$$\Delta f \cong \frac{1}{2\pi\rho_q t_q} t_f \rho_f \omega \left(1 + \frac{2t^2\chi}{3\delta^2(1+\chi^2)}\right) \quad (2)$$

$$\Delta D \cong \frac{2t^3\rho_f f}{3\pi f_{ro}\rho_q t_q} \frac{1}{\delta^2(1+\chi^2)} \quad (3)$$

where ρ_q and ρ_f are the densities of the quartz and film, respectively; t_q and t_f are the thicknesses of the quartz and film, respectively; and χ is the inverse of the mechanical loss tangent (tan δ) and is equal to the ratio of the storage modulus (μ_f) to the loss modulus (η_f). Using four different overtones and eqs 2 and 3, we fit changes in the frequency and dissipation to the film viscosity (η_f), shear modulus (μ_f), thickness (t_f), and density (ρ_f). Overtones were fitted to this model using the commercial program Q-tools software (Q-sense AB).[38,41]

Atomic Force Microscopy (AFM) Imaging. AFM experiments were carried out on a MFP-3D-BIO Atomic Force Microscope (Asylum Research, Santa Barbara, CA) operated in tapping mode. Microcantilevers from Biolever (Olympus, Tokyo, Japan) were used for all measurements; they have a force constant of $k = 0.32$ N·m^{-1} or $k = 0.06$ N·m^{-1} and a nominal tip radius of 10 nm. All measurements were performed in Tris buffer (150 mM NaCl, 10 mM Tris, 1 mM EDTA, pH 7.5. Samples were maintained in a closed fluidic cell. Igor Pro software (Wave Metrics, Lake Oswego, OR) was used for image flattening and data analysis of the TM-AFM images.

Fluorescence Recovery after Photobleaching (FRAP) Measurements. All fluorescence measurements were performed with a Leica Spectral Confocal and Multiphoton microscope (Wetzlar, Germany) using the 561 nm line as the source for both bleaching and monitoring fluorescence recovery. To obtain the fluorescence images, Texas Red- DHPE (0.5%, w/w) was incorporated as a tracer into the POPC/DP-NGPE vesicles. The diameter of the bleached spot was 15 μm and the bleaching time was ~30 s. The data were analyzed by Metamorph software. The theoretical data analysis was performed as described by Axelrod et al.[42] For convenience, fluorescence recovery curves are displayed in fractional form, $f_k(t)$, and defined as follows:

$$f_k(t) = \frac{F_k(t) - F_k(0)}{F_k(\infty) - F_k(0)} \quad (4)$$

where $F_k(t)$ is the integrated fluorescent intensity observed at time $t \geq 0$. In addition, the diffusion coefficient, D, was related to the half-life of this recovery:

$$D = r^2/4\tau \quad (5)$$

where r is the radius of the bleached spot and τ is the time for half recovery of the fractional integrated fluorescent intensity. Mobility data are reported as the mean of at least five separate experiments.

Results

Adsorption Kinetics of Type I Collagen Conjugation on a Supported Lipid Bilayer as Monitored by QCM-D. Collagen is a key component of the extracellular matrix (ECM) and is linked to cell membranes via integrins,[43] as shown in Scheme 1a. To mimic the natural ECM environment to encourage cell growth, we constructed a collagen matrix via chemical synthesis on a supported lipid bilayer. Triple helical type I collagen (~300 kD) consists of 35% glycine, 11% alanine, 21% proline, and hydroxyproline.[44] Of the remaining amino acids, primary amine groups on the lysine residues can be utilized for chemical coupling. We converted the carboxylic acid groups on the DP-NGPE lipids to NHS-ester groups by EDC/sNHS treatment.[31–34] After the DP-NGPE lipids were functionalized (abbreviated as NHS-DP-NGPE), POPC/NHS-DP-NGPE vesicles formed a functionalized supported lipid bilayer on SiO_2, and type I collagen was subsequently coupled to the functionalized lipid bilayers.

Scheme 1. Pictorial Representation of Mimetic Collagen Binding Strategy Based on Integrins in Biologic Cells: (a) Cells Bind Collagen Fibers via Integrins; (b) Collagen Fibers are Chemically Conjugated onto the Model Lipid Membrane. The Olive Pentagons Represent the NHS-Ester Groups of DP-NGPE and the Blue Spheres Symbolize POPC Headgroups

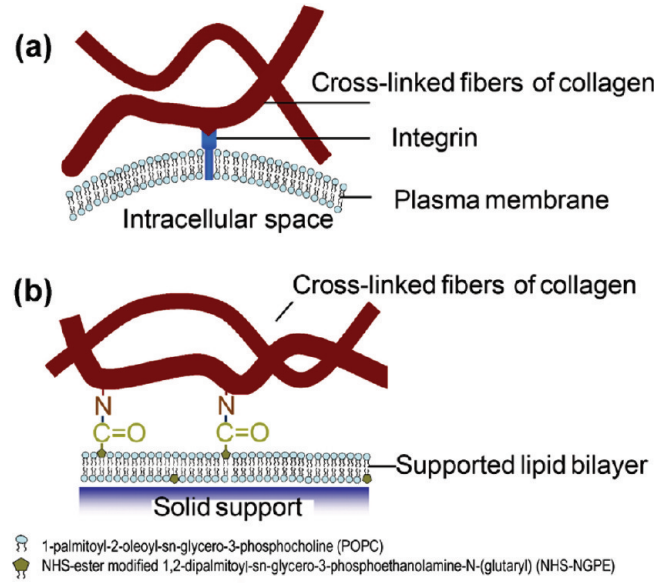

To fabricate the collagen-conjugated supported lipid bilayer system, we first created the functionalized bilayer platform, as shown in Scheme 1b. Our system demonstrated typical vesicle fusion kinetics in terms of QCM-D frequency and dissipation responses as shown in Figure 1a, which are in good agreement with past results.[21,36–38,45,46] Following initial stabilization of the frequency and dissipation responses in buffer solution for 5 min, a 90% POPC/10% NHS-DP-NGPE lipid vesicle solution was added (point V). Two-step kinetics was observed, and the final frequency and dissipation values after buffer washes (B_1 and B_2) were in good agreement with previous observations on complete planar bilayers ($\Delta f \sim 26$ Hz and $\Delta D \sim 0 \times 10^{-6}$, respectively).[21,47] To ensure the consistency of the cell culture platform, we only studied supported lipid bilayers with up to 40% NHS-DP-NGPE (see Supporting Information for further vesicle fusion QCM-D kinetics of different lipid compositions). For vesicles whose NHS-DP-NGPE lipid composition was greater than 40%, the final frequency and dissipation values suggested that the bilayers were incomplete planar bilayers (Supporting Information, Figure S1).

After forming the supported lipid bilayer, the type I collagen solution was introduced (Figures 1b and 2, symbol C). Of note, as depicted in Figure 2, the frequency and dissipation changes associated with type I collagen binding onto lipid platforms functionalized with different concentrations of NHS-DP-NGPE demonstrated that collagen binding is strongly dependent on the concentration of NHS-DP-NGPE functionalized lipid (see the plotted time from 35 to 130 min in Figure 2). The significant frequency response decrease indicates collagen adsorption onto

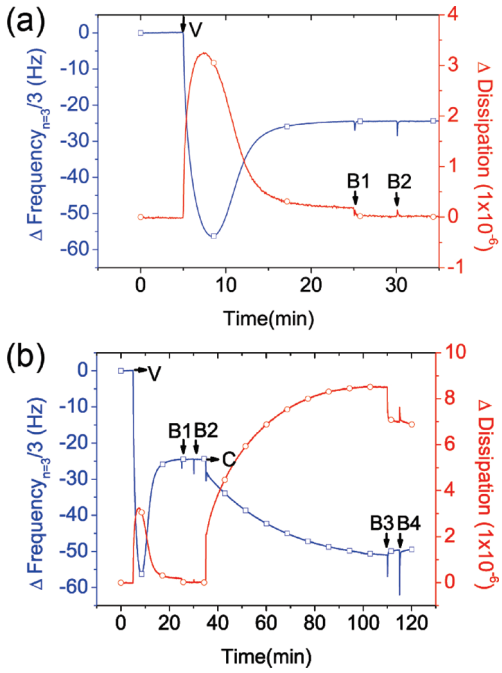

Figure 1. Typical QCM-D experiment in which collagen-conjugated lipid bilayers are constructed by vesicle fusion. The open blue squares indicate frequency changes ($n = 3$), and the open red circles indicate the changes in energy dissipation. (a) The formation of a POPC/NHS-DP-NGPE 10% supported lipid bilayer on SiO_2 by vesicle fusion (V) is followed by Tris buffer washes (B1, B2); (b) Collagen is injected (C) into the chamber using the same platform as in Figure 1 (a). Subsequently, the collagen is rinsed by Tris buffer (B3, B4) to eliminate unbound collagen molecules and stabilize the signals.

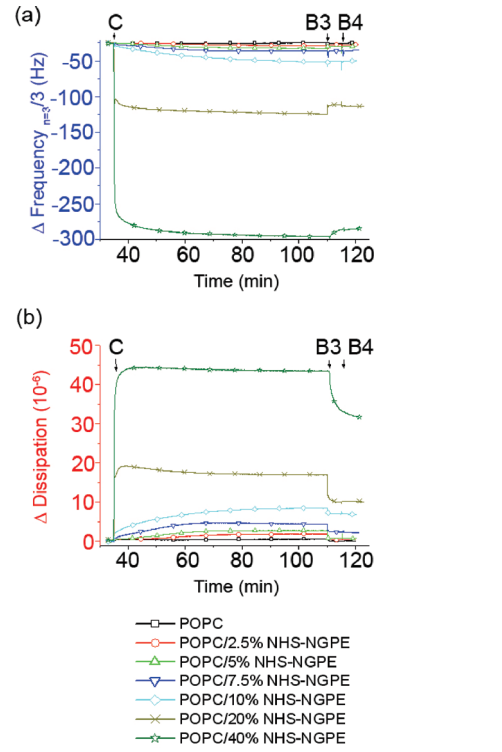

Figure 2. QCM-D kinetics for the conjugation of collagen on functionalized lipid bilayers. (a) Changes in frequency for functional lipid bilayers of varied NHS-DP-NGPE concentration after addition of collagen solution at point C. We washed with Tris buffer twice to remove the unbound collagen and monitor the stabilization of the signals. (b) The corresponding changes of dissipation for functional lipid bilayers of varied NHS-DP-NGPE concentration.

the functionalized supported bilayer. After a period of rapid initial binding, collagen adsorption took place slowly over the course of 100 min, with the dissipation response increase revealing the adsorbed collagen's high degree of viscoelasticity. Both Δf and ΔD values changed after subsequent Tris buffer washes at points B3 and B4, which suggests the removal of loosely bound collagen that could in turn affect the orientation of remaining bound collagen molecules.

The collagen binding capacity was modulated by changing the percentage of NHS-DP-NGPE in the vesicles from 0 to 40%, as shown in Figure 2. As a control experiment, we examined collagen adsorption onto a supported POPC lipid bilayer (POPC square with black line). As expected, we did not observe any collagen adsorption onto the control. This result agrees well with previous studies, which indicate that nonfunctionalized supported lipid bilayers are "non-stick" to collagen adsorption.[48,49] Furthermore, bilayers consisting of up to 5% of DP-NGPE without EDC/sNHS activation (data not shown) showed no evidence of collagen binding. We then increased the NHS-DP-NGPE concentrations from 2.5 to 40%. As we increased the NHS-DP-NGPE concentration in the bilayer platform, we were able to observe corresponding decreases in frequency and increases in dissipation. These responses demonstrate that type I collagen binding can occur due to EDC/sNHS activation and is a function of the percentage of functionalized lipids in the supported bilayer.

The most striking result for binding stability was observed after the collagen-functionalized bilayers were washed twice with buffer. We were able to identify two different kinetic processes after Tris buffer washing: (A) For bilayers containing 10% of NHS-DP-NGPE or less, desorption (i.e., removal of unbounded collagen) was observed, as indicated by the corresponding increase in Δf, although the changes were relatively minor in magnitude; (B) By contrast, for bilayers containing at least 20% NHS-DP-NGPE, the increase in Δf and decrease in ΔD were larger and occurred over a 10 min period. This longer period of stabilization may be due to not only the removal of unbounded collagen but also an effect on the remaining bound collagen's molecular organization.

Morphology and Molecular Organization of Collagen Structure Imaged by TM-AFM. TM-AFM measurements were performed to examine the morphological structure of the adsorbed collagen molecules as well as the supported lipid bilayer underneath. We recorded TM-AFM height images of adsorbed collagen on mica-supported functionalized bilayers to understand the structural configuration of the conjugated collagen molecules and to verify the height of the underlying bilayer (Figure 3a,b).

Similar to the QCM-D experiments, we first constructed a functionalized supported lipid bilayer by the vesicle fusion process, whereby vesicles spontaneously adsorb onto a hydrophilic mica surface and eventually rupture after reaching a critical coverage. A defect of the lipid bilayer on the mica surface was imaged, permitting us to check the thickness of the lipid bilayer, which was about 4.5 nm (Supporting Information, Figure S2). As a control experiment, Figure 3a shows that the morphology of an inactivated functionalized lipid bilayer, after immersion in a collagen solution, has a similar surface roughness to that of a bare lipid bilayer (Supporting Information, Table S1), demonstrating that collagen does not adsorb on a chemically inactivated DG-NGPE surface. Further, no phase separated lipid domains were found although the dipalmitoyl (DP) form of NGPE lipids contains two saturated long-carbon

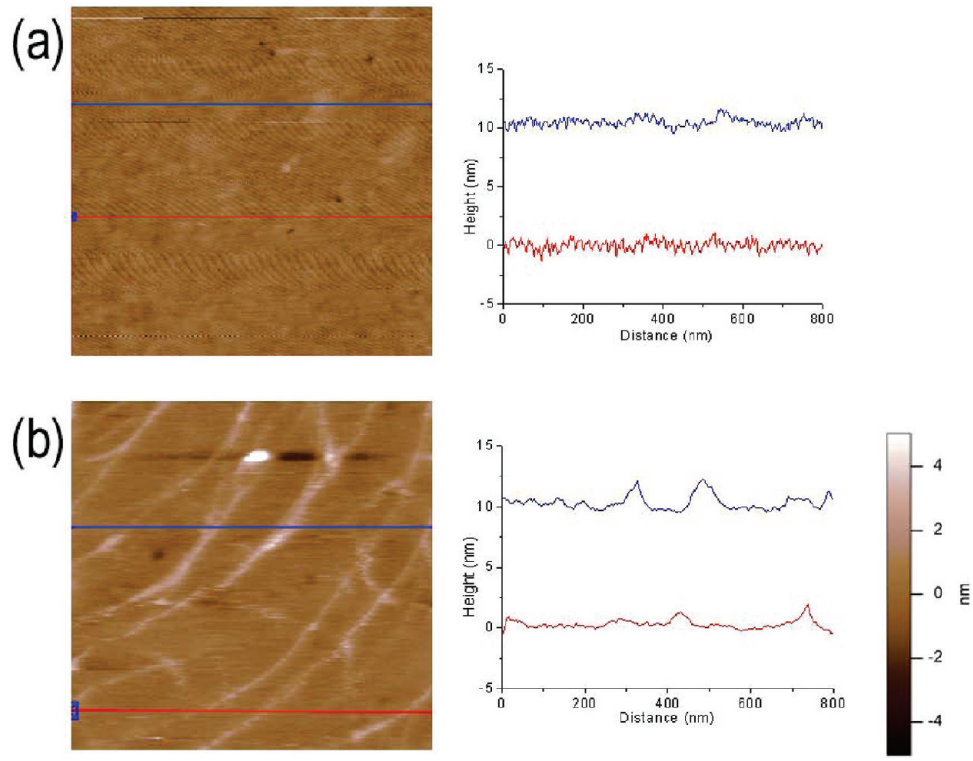

Figure 3. TM-AFM height images of adsorbed collagen adlayers on lipid bilayers with (a) unactivated DP-NGPE and (b) 20% NHS-DP-NGPE. Bar size: 100 nm. Z-scale: 10 nm. The image size is 800 × 800 nm. In addition, we also present two different cross-sectional profiles for each image.

chains (both 16:0) and POPC lipids have a more disordered chain structure (16:0 and 18:1). When the NHS-DP-NGPE lipid percentage was increased to 20%, as shown in Figure 3b, large collagen fibrils formed on top of the lipid bilayer surface; the length of these fibrils reached the order of 1 μm. These results suggest that the aggregated state of collagen changes with the surface binding density. The TM-AFM study proved to be complementary to the QCM-D study because it provided both quantitative analysis of collagen adsorption and revealed insight into adsorbed collagen morphology as a function of the amine-NHS lipid density within the bilayer.

Influence of Adsorbed Collagen on the Lateral Mobility of Functionalized Lipid Bilayers. Because of the introduction of the fluid mosaic model,[50] which envisioned the cell membrane as a two-dimensional fluid matrix, the fluidity of cell membranes has become well-recognized, and thus, lipid mobility is an important parameter for model membrane systems.[51] Therefore, we explored the ability of lipids in the functionalized bilayer with and without adsorbed collagen to laterally diffuse by using the FRAP technique. Figure 4 demonstrates typical fluorescence recovery images with quantitative line scans acquired from bilayers consisting of 90% POPC and 10% NHS-DP-NGPE with and without collagen. Fluorescence recovery occurred, as indicated by the redistribution of red dye to the central bleached spot over a period of 30 min. The fluorescent profiles were normalized with respect to each bleached spot. For bilayers without bound collagen (Figure 4a), recovery was fast and relatively complete. Bound collagen acted as an obstacle to diffusion and the lateral lipid mobility of the bilayers became dramatically hindered, resulting in substantial recovery of the bleached area for collagen-conjugated bilayers taking up to 30 min (Figure 4b).

Based on the FRAP experiments, the lateral lipid mobility of the POPC/ NHS-DP-NGPE lipid bilayers could be quantitatively estimated by the diffusion coefficient, D, according to eq 5. To account for changing bilayer mobility upon collagen binding only, we used relative diffusivity, D^* (dimensionless) such that $D^* = D_c/D_0$, where D_c and D_0 are the diffusion coefficients of individual lipid bilayers of specific lipid composition, measured in the presence (D_c) and absence (D_0) of bound collagen. The values of D_c, D_0, and D^* of the samples are plotted versus the initial percentages of NHS-DP-NGPE in Figure 5. As a control experiment, we calculated the relative diffusion coefficient D^* of pure POPC without DP-NGPE (i.e., 99.5% POPC mixed with 0.5% Texas Red PE) in the presence of collagen. The calculated value of approximately one demonstrated that collagen has no effect on lipid mobility in the absence of functionalized lipids.

To assess the quality of the functionalized lipid bilayers, we first checked the mobility of lipid bilayers without bound collagen as a function of DP-NGPE concentration, as shown in Figure 5. As the bilayer contained an increasing amount of DP-NGPE, there was a decrease in lipid lateral mobility. These significant decreases were expected because the dipalmitoyl (DP) form of the NGPE lipid, which contains two saturated long-carbon chains, has a higher gel−liquid chain melting (phase transition) temperature (T_c) than POPC lipids ($T_c \sim 41$ °C vs −10 °C), which have one unsaturated chain. Although we did not detect the presence of microscopic phase-separated lipid domains with AFM, there is the possibility that the likely immiscibility of these two lipids could result in the formation of nanoscopic domains that act as diffusion barriers.[52] Accordingly, lateral lipid diffusivity in the POPC/NHS-DP-NGPE bilayer was lower than the diffusivity in the pure POPC bilayer. The relative diffusion coefficient decreased from 1.0 to 0.2 as the concentration of NHS-DP-NGPE in the bilayer increased from 0 to 40%. This may explain why lateral lipid mobility is often an order of magnitude slower in cell membranes than in model membrane systems.

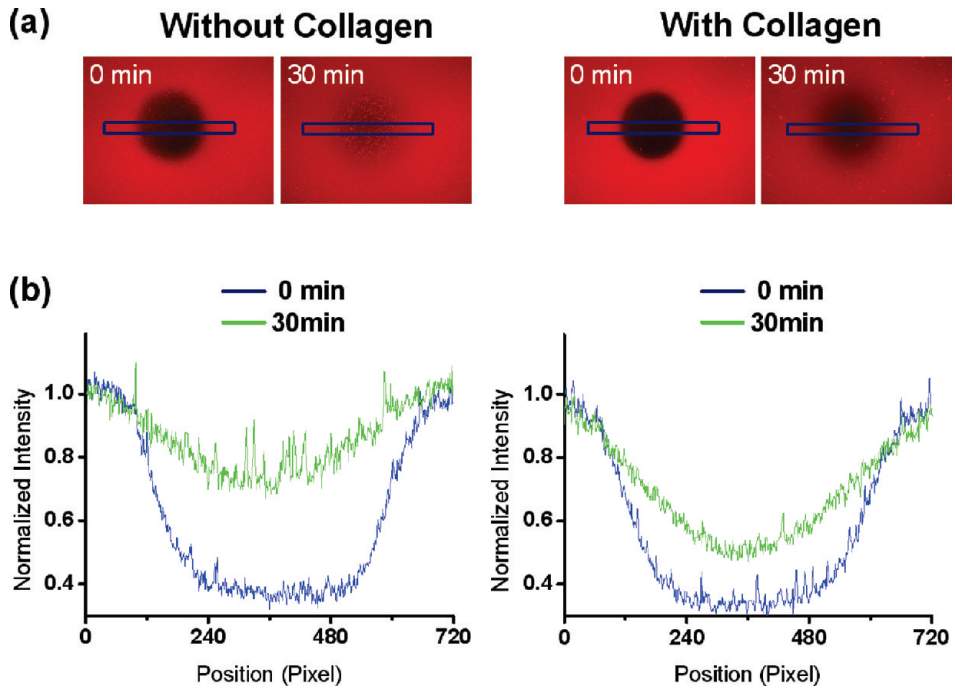

Figure 4. (a) Microscopic images showing the recovery of a bleached spot on 10% NHS-DP-NGPE lipid bilayers with and without collagen. (b) Quantitative traces of normalized fluorescence intensity across the bleached spot at 0 and 30 min.

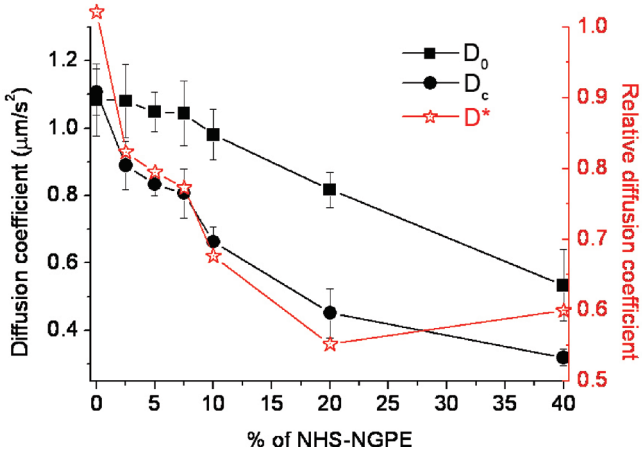

Figure 5. Influence of NHS-DP-NGPE lipid percentage on the relative diffusion coefficient, D^* (red stars, right axis), and diffusion coefficients, D_c (black circles, left axis) and D_0 (black squares, left axis), measured in the presence and absence of collagen, respectively, by FRAP.

A10 Vascular Smooth Muscle Cells (SMCs) Spreading on Collagen-Functionalized Lipid Bilayers. Our goal is to apply this platform to study cell−ECM interactions in the presence of an underlying lipid bilayer. Previous studies have demonstrated that a type I collagen-enriched extracellular matrix is highly regulated by integrin engagement, which further maintains the proliferation of vascular smooth muscle cells in the differentiated state.[53,51] Therefore, we investigated the growth behavior of vascular smooth muscle cells (A10) on functionalized lipid bilayers in both the presence and absence of type I collagen in DMEM medium with 10% serum. The resulting bright field images demonstrated that fewer A10 cells can survive and locally spread on lipid bilayers without collagen (Figure 6a) as compared to collagen-conjugated bilayers (Figure 6b), which supported higher cell growth levels that are in good agreement with results obtained on culture dishes. Quantitative analysis based on the image results show that a 2.5 times higher average cell population (~1000 cell counts/mm^2) and a 6 times larger spreading area of smooth muscle cells (~800 μm^2) are present on the type I collagen-modified bilayer than those on the bare bilayer surface. Thus, conjugated type I collagen maintains the growth and adhesion of smooth muscle cells on the lipid bilayer platform.

Discussion

Collagen Molecular Organization as Analyzed by QCM-D and TM-AFM. The phospholipid bilayer is a common molecular architecture that mimics the cell membrane for potential biosensor and biochip applications.[2,3,54] However, a bare lipid bilayer is considered a nonbiofouling surface that is resistant to both protein adsorption and cell adhesion.[46,47,53] This phenomenon has been explained by several models based on hydrophilicity,[56–59] surface polarizability,[46,47,53] and the thickness of the separating water layer.[55] There is growing attention to develop a biomimetic platform that provides specific regions to bind cells for tissue engineering applications.[53–55]

Herein, we designed a biomimetic assembly by a bottom-up approach that incorporated functionalized molecular building blocks based on EDC/NHS-chemistry onto a supported bilayer platform to chemically tether type I collagen. Type I collagen is a complex macromolecule consisting of multiple binding domains for self-polymerization, resulting in the formation of aggregates ranging from small filaments to large fibrils with dimensions ranging from 100 nm to a few μm.[56] The polymerization of type I collagen on a substrate is often controlled by physical parameters such as concentration, pH, and temperature, and in some cases, it depends on the presence of fibronectin and integrins as well.[30]

To analyze the assembly behavior of the type I collagen molecules upon binding to the functionalized lipid bilayer, we characterized the viscoelastic changes caused by surface-bound collagen by plotting ΔD as a function of Δf (Figure 7). These data, recorded upon exposure of collagen to functionalized lipid bilayers, demonstrate the viscoelastic changes caused by adsorbed collagen layers. The slopes of the lines defining collagen

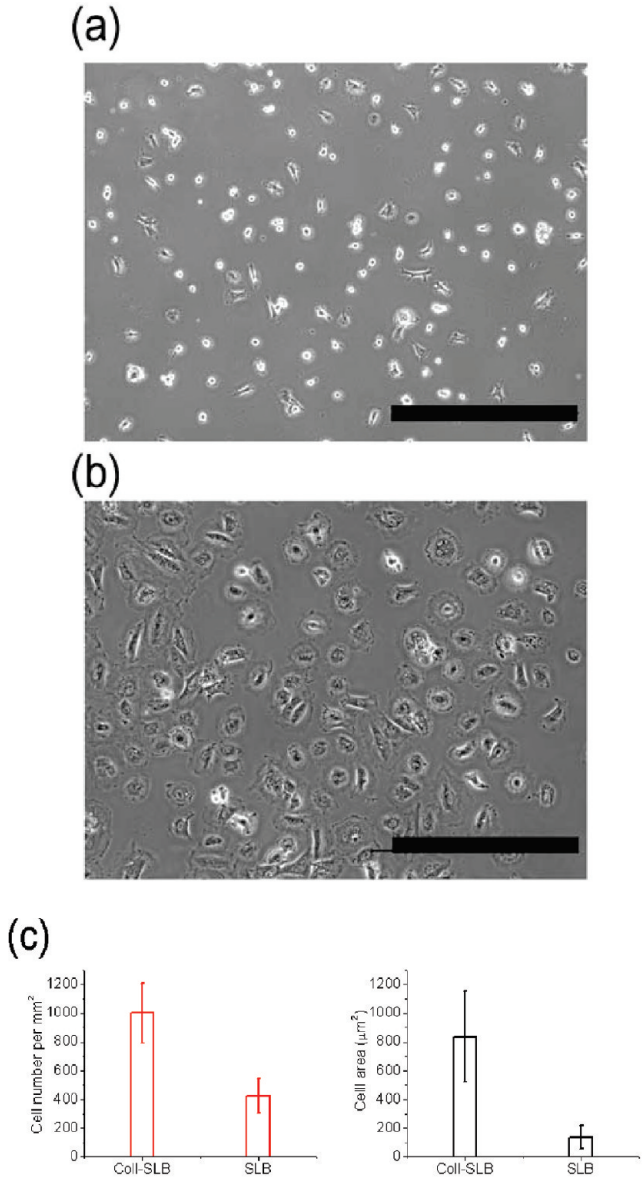

Figure 6. Cell growth on collagen-conjugated lipid bilayer culture platforms. Microscopic images of smooth muscle cells A10 cultured on lipid bilayers containing 20% NHS-DP-NGPE that were either (a) without collagen or (b) functionalized with collagen in DMEM medium with 10% serum overnight. The scale bars are 100 μm. (c) The cell number (red bars, left panel) and cell spreading area (black bars, right panel) were estimated by Metamorph software based on the image collection.

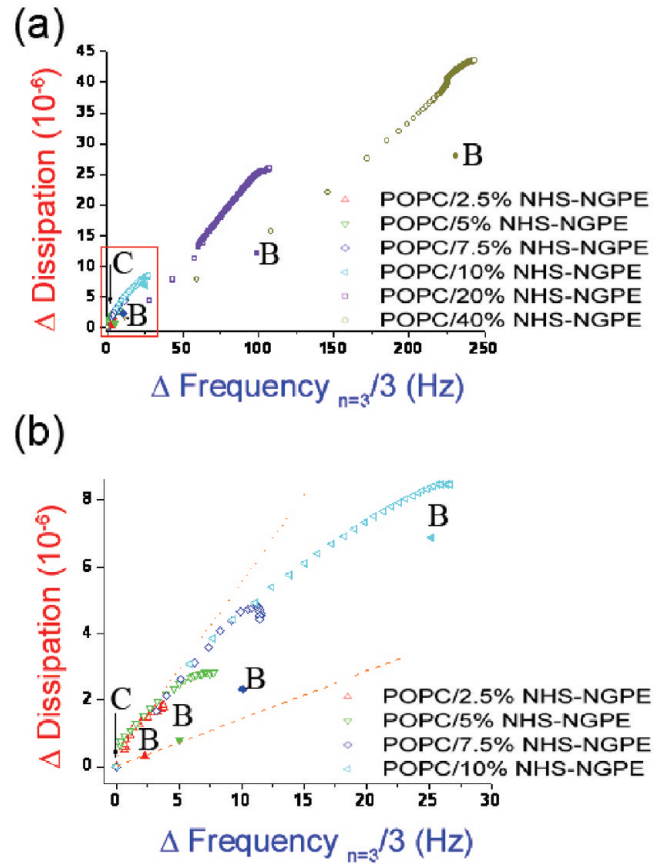

Figure 7. Δf-ΔD curves for different concentrations (w/w %) of NHS-DP-NHPE in functionalized lipid bilayers. Data is replotted from Figure 2 so that time is an implicit variable. Open symbols labeled C represent values after the addition of collagen solution. Solid symbols labeled B depict the values after subsequent washing steps with Tris buffer. (a) Collagen adsorption kinetics for NHS-DP-NGPE concentration range from 2.5−40%. (b) Magnified view of red box in part (a). The ellipses (•••) show a linear fit to the 2.5% NHS-DP-NHPE curve before buffer wash, and the dashes (---) show a linear fit to the 2.5% NHS-DP-NGPE curve after two washing steps. Adsorption was measured for 75 min, and the absolute Δf at $n = 3$ was normalized to 25 Hz.

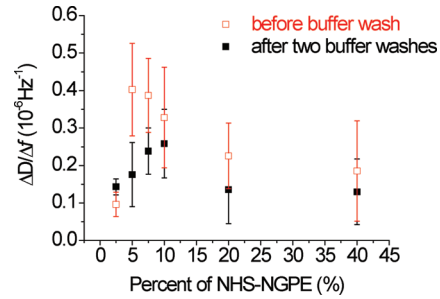

Figure 8. Ratio of energy dissipation changes to frequency changes for collagen adlayers on functionalized lipid bilayers containing various percentages of NHS-DP-NGPE.

adsorption kinetics on the lipid bilayers with higher percentages of NHS-DP-NGPE are less than for the bilayers with lower percentages. This type of analysis has proven useful when comparing vesicle and bilayer adsorption kinetics because time becomes an implicit parameter.[57] By characterizing the slope of ΔD as a function of Δf, we are able to monitor the changes in viscoelastic properties for adlayers such as collagen. The slope difference represents the change in the molecular conformation, as indicated by the different viscoelastic states, of the collagen adsorbed onto functionalized lipid bilayers with various percentages of NHS-DP-NGPE. We also compared the ratio of change in energy dissipation to the change in frequency as a function of the change in NHS-DP-NGPE percentage. The change in dissipation is related to the morphological behavior of collagen and the change in frequency is proportional to the increase of adsorbed collagen mass on the functionalized lipid bilayer. The ratio of these changes serves as an indicator of the viscoelastic nature of the adlayer on functionalized lipid bilayers. When comparing the free equilibrium state (before buffer washing) of the collagen adlayers, we found that with increasing concentration of NHS-DP-NGPE, the ratio $\Delta D/\Delta f$ (10^{-6} Hz^{1-}) decreased from 0.4 to 0.23 (Figure 8). This decrease is attributed to the attractive forces exerted by NHS-DP-NGPE. After buffer washing, we observed that on lipid bilayers containing between 10% and 20% NHS-DP-NGPE, the collagen undergoes a conformational transition. Up to 10% NHS-DP-NGPE, the

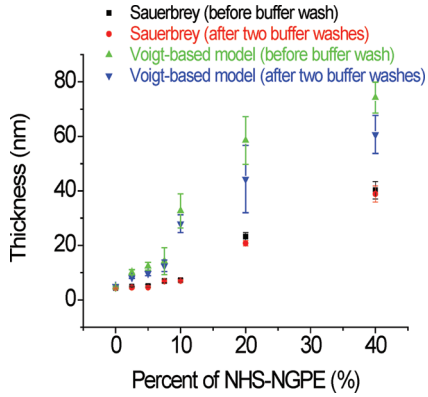

Figure 9. Adlayer thicknesses determined by the Sauerbrey and Voigt models. The Sauerbrey thicknesses before buffer wash and after two buffer washes are indicated by black squares and red circles, respectively. The Voigt thicknesses before buffer wash and after two buffer washes are represented by green and blue triangles, respectively.

repulsive forces may play a role that promotes collagen molecules to assume a more viscoelastic state. At 20% NHS-DP-NGPE, the attractive forces (chemical force exerted by NHS-DP-NGPE) are dominant so the adsorbed collagen collapses. The buffer washes effectively removed nonspecifically bound collagen molecules and seem to further enhance the molecular assembly process. Interestingly, when compared with the experimental data of collagen on polystyrene (PS) plates, which is generally considered to be a surface dominated by attractive forces, the viscoelastic nature of the adsorbed collagen adlayer ($\Delta f = 188.17$ Hz and $\Delta D = 19.99 \times 10^{-6}$) was similar to that on the functionalized lipid bilayers with 40% NHS-DP-NGPE. This observation supports our conclusion that, at high percentages of NHS-DP-NGPE in the lipid bilayer, the repulsive force is negligible.

We further examined the changes in thickness of the adsorbed collagen adlayers obtained by the QCM-D measurements (Figure 9) by employing both the Sauerbrey equation (eq 1) and the Voigt-based model.[58] Throughout our calculations, we assumed a homogeneous film thickness and the density of the adlayer to be 1200 kg·m^{-3}. Although the fundamental assumption of the Sauerbrey equation is that the adlayer is a homogeneous foreign mass with a spatially uniform density and rigid solid state, our experiments showed that the adlayer displayed relatively large energy dissipation. For this reason, we also employed the Voigt-based viscoelastic model, which is a better fit for collagen−lipid bilayer systems. We utilized the fifth, seventh, and ninth overtones to calculate the Voigt thickness as shown in Figure 9. For a detailed discussion of the Voigt model calculations, the reader is referred to ref 38 and references therein.

Our Voigt-based simulation demonstrated that the thickness of the adsorbed collagen adlayer increased with the amount of adsorbed collagen, similar to the results from the Sauerbrey equation. The huge thickness discrepancy (more than ~20 nm) between the Sauerbrey and Voigt-based model occurred from 10% NHS-DP-NGPE onward and was mainly caused by energy dissipation changes due to the viscoelasticity of the collagen adlayer. Specifically, after two buffer washes, the Sauerbrey and Voigt collagen thicknesses decreased over 50% for those samples containing at least 20% NHS-DP-NGPE. With 10% NHS-DP-NGPE or less, we did not see any deviation after two buffer washes. The thickness transition between 10 to 20% NHS-DP-NGPE coincides with the previous prediction.

In order to further analyze the molecular organization of the collagen upon adsorption onto the functionalized lipid bilayer, TM-AFM images provided insight into the topography of the collagen adlayer on the functionalized lipid bilayer. The size and morphology of collagen aggregates on functionalized lipid bilayers with NHS-DP-NGPE percentages less than 20% were not in agreement with those on PS,[14,67,68] poly(ethylene terephthalate) (PET),[59] and CH_3-terminated self-assembled monolayers (SAM),[60] on which collagen molecules have entire adhesion sites for coverage and develop fibrillar structures during adsorption. By increasing the percentage of NHS-DP-NGPE to 20%, however, long collagen fibrils were formed on top of the lipid bilayer.

For the 80% POPC/20% NHS-DP-NGPE bilayer, the TM-AFM images show that the collagen fibrils are ~8 nm thick. From the QCM-D modeling estimate of this composition, the average thickness of the collagen adlayer ranged from 35 to 56 nm (see Figure 9, after two buffer washes). The much smaller thickness measured by TM-AFM is possibly due to tip effects.[58,59] In addition, the TM-AFM images showed that the collagen fibrils form a heterogeneous adlayer. Thus, there could also be some variation between the thicknesses obtained from the QCM-D models, which assume a homogeneous and uniform adlayer, and the nonuniform sample thickness. Nonetheless, the results obtained from both QCM-D modeling (Figure 9) and TM-AFM imaging (Figure 3, Figure S3) provide consistent trends in terms of the relationship between collagen thickness and surface binding density.

Taken together, the QCM-D and TM-AFM images indicate that material properties such as viscoelasticity and the thickness of the collagen adlayer are related to the formation of collagen fibrillar structures and to the propensity to bind to functionalized lipid bilayers. In this study, we verified the feasibility of cell culture on this protein-conjugated lipid bilayer surface and showed that cells can grow on a collagen-functionalized supported lipid bilayer platform. Cell spreading area and adherent number illustrate the fact that cell growth is tightly associated with the communication between cellular receptors and ECM materials. By adjusting the percentage of NHS-DP-NGPE, which acts as a mimic for receptors such as integrins on cell membranes, we may modulate the biological activity between the cell membrane and ECM components in a targeted way.

Restriction on Mobility of Supported Lipid Bilayers by Adsorbed Collagen. The relationship between molecular composition in solid-supported lipid bilayers and lateral diffusion of targeted lipids or proteins has been extensively investigated by FRAP.[24,61−64] After photobleaching, the fluorescent images showed a substantial fluorescence recovery of Texas Red-PE lipids embedded into binary lipid bilayers coupled with and without collagen (Figure 4a). The fluorescence recovery confirms the lateral diffusion mobility of the lipid molecules and is also used to verify bilayer formation.

The quantitative analysis of normalized fluorescence across the photobleached spot (Figure 4b) revealed that the conjugation of collagen molecules on lipid bilayers slowed the lipid mobility. The reduction in diffusion mobility associated with macromolecules being bound on the lipid bilayer was in good agreement with other reports showing supported bilayer architectures associated with macromolecular adsorption including tethered vesicles,[61] annexin-phospholipid complexes,[62,63] CTB-G_{M1} binding,[64] and membrane protein insertion,[24] which displayed similarly significant reduction in diffusivity when coupling occurred. In addition, the polymer-supported bilayers using covalent binding to solid[65] and polymer-adsorbed bilayers by polyelectrolytes[52,66] hindered diffusion in both outer and inner membrane leaflets.

In biological systems, multiple factors, including membrane folding, lipid composition, cytoskeleton activity, and membrane protein ratio,[67] can cause an order of magnitude slower lateral lipid diffusion rate in biomembranes. In Figure 5, on a diluted collagen-conjugated lipid bilayer (2.5% NHS-DP-NGPE), the lateral lipid mobility dropped by 20% ($D^* = 0.78$). This phenomenon demonstrated that a small amount of collagen binding could cause a reduction in lipid diffusion mobility. Further, the mobility of the collagen-conjugated lipid bilayers with 40% NHS-DP-NGPE was reduced by almost 50%, supporting the view that decreased mobility is caused by conjugated collagen molecules.

Another point to consider in the case of the 40% DP-NGPE bilayer is the effects of the vesicle rupturing kinetics to form the supported bilayer. The presence of some adsorbed vesicles on the substrates might also play a role in the significant retardation of lateral diffusion. Nonetheless, there is clear evidence that the physical hindrance[65] caused by collagen binding significantly reduces bilayer mobility. Based on our findings, including the characterization of a novel, collagen-functionalized supported lipid bilayer platform and its success as a cell culture platform, we present this biomimetic platform as an ECM-mimic for promoting cell growth and for studying ECM-cell interactions.

Conclusions

In this paper, we have successfully fabricated a novel molecular assembly based on a solid-supported lipid bilayer conjugated with an ECM protein by a bottom-up approach. EDC/NHS chemistry was used to covalently bind an ECM protein, type I collagen, onto a supported lipid bilayer. QCM-D was employed to determine the binding kinetics and resultant changes in thickness and viscoelasticity of the adsorbed collagen adlayer. AFM was applied to obtain morphological evidence that adsorbed collagen fibers form fibrillar structures under certain conditions. Further, FRAP experiments were performed to monitor the bilayer fluidity before and after collagen adsorption. Finally, A10 vascular smooth muscle cells were successfully cultured on functionalized lipid bilayers in the presence of type I collagen.

The current proposed system is a simple bottom-up biomimetic strategy, which contains key constituents of the plasma membrane and the extracellular matrix (ECM) of cellular systems. One can easily expand this platform and create more complex biomimetic systems by assembling more biologically specific components or introducing a set of multifaceted molecules such as fibronectin and integrins. This strategy potentially facilitates the study of how cells recognize and respond to specific extracellular matrix elements and can provide valuable information about cell−membrane interactions.

Acknowledgment. This work was funded by Academia Sinica, Taipei, Taiwan, and the QCM-D experiments were performed in the Center on Polymer Interfaces and Macromolecular Assemblies (CPIMA), Stanford University, Stanford, CA. We thank Dr. Kay Kanazawa for his valuable comments on QCM-D analysis and Ankit Patel for technical support.

Supporting Information Available. (Figure S1) Complete bilayer formation with different percentages of NHS-DP-NGPE on SiO_2 solid support; (Figure S2) Bilayer formation on mica by TM-AFM. This material is available free of charge via the Internet at http://pubs.acs.org.

References and Notes

(1) Sapora, O.; Di Carlo, B. Cell signaling mechanisms and the control of cell life and death. *Radiat. Prot. Dosim.* **2006**, *122* (1−4), 210–20.
(2) Sackmann, E.; Tanaka, M. Supported membranes on soft polymer cushions: fabrication, characterization and applications. *Trends Biotechnol.* **2000**, *18* (2), 58–64.
(3) Sackmann, E. Supported membranes: scientific and pratical applications. *Science* **1996**, *271*, 43–48.
(4) Chen, C. S.; Mrksich, M.; Huang, S.; Whitesides, G. M.; Ingber, D. E. Geometric control of cell life and death. *Science* **1997**, *276* (5317), 1425–1428.
(5) Koyama, H.; Raines, E. W.; Bornfeldt, K. E.; Roberts, J. M.; Ross, R. Fibrillar collagen inhibits arterial smooth muscle proliferation through regulation of Cdk2 inhibitors. *Cell* **1996**, *87* (6), 1069–1078.
(6) Lutolf, M. P.; Hubbell, J. A. Synthetic biomaterials as instructive extracellular microenvironments for morphogenesis in tissue engineering. *Nat. Biotechnol.* **2005**, *23* (1), 47–55.
(7) Dankers, P. Y. W.; Harmsen, M. C.; Brouwer, L. A.; Van Luyn, M. J. A.; Meijer, E. W. A modular and supramolecular approach to bioactive scaffolds for tissue engineering. *Nat. Mater.* **2005**, *4* (7), 568–574.
(8) Feng, Y. Z.; Mrksich, M. The synergy peptide PHSRN and the adhesion peptide RGD mediate cell adhesion through a common mechanism. *Biochemistry* **2004**, *43* (50), 15811–15821.
(9) Chowdhury, E. H.; Nagaoka, M.; Ogiwara, K.; Zohra, F. T.; Kutsuzawa, K.; Tada, S.; Kitamura, C.; Akaike, T. Integrin-supported fast rate intracellular delivery of plasmid DNA by extracellular matrix protein embedded calcium phosphate complexes. *Biochemistry* **2005**, *44* (37), 12273–12278.
(10) Allen, T. D.; Schor, S. L.; Schor, A. M. An ultrastructural review of collagen gels, a model system for cell-matrix, cell−basement membrane and cell−cell interactions. *Scan Electron Microsc.* **1984**, (Pt 1), 375–90.
(11) Kadler, K. E.; Hojima, Y.; Prockop, D. J. Assembly of collagen fibrils de novo by cleavage of the type-1 pc-collagen with procollagen c-proteinase-assay of critical concentration demonstrates that collagen self-assembly is a classical example of an entropy-driven process. *J. Biol. Chem.* **1987**, *262* (32), 15696–15701.
(12) Kadler, K. E.; Holmes, D. F.; Graham, H.; Starborg, T. Tip-mediated fusion involving unipolar collagen fibrils accounts for rapid fibril elongation, the occurrence of fibrillar branched networks in skin and the paucity of collagen fibril ends in vertebrates. *Matrix Biol.* **2000**, *19* (4), 359–365.
(13) Mrksich, M.; Dike, L. E.; Tien, J.; Ingber, D. E.; Whitesides, G. M. Using microcontact printing to pattern the attachment of mammalian cells to self-assembled monolayers of alkanethiolates on transparent films of gold and silver. *Exp. Cell Res.* **1997**, *235* (2), 305–313.
(14) Elliott, J. T.; Woodward, J. T.; Langenbach, K. J.; Tona, A.; Jones, P. L.; Plant, A. L. Vascular smooth muscle cell response on thin films of collagen. *Matrix Biol.* **2005**, *24* (7), 489–502.
(15) Cluzel, C.; Saltel, F.; Lussi, J.; Paulhe, F.; Imhof, B. A.; Wehrle-Haller, B. The mechanisms and dynamics of alpha v beta 3 integrin clustering in living cells. *J. Cell Biol.* **2005**, *171* (2), 383–392.
(16) Mossman, K. D.; Campi, G.; Groves, J. T.; Dustin, M. L. Altered TCR signaling from geometrically repatterned immunological synapses. *Science* **2005**, *310* (5751), 1191–1193.
(17) Pautot, S.; Lee, H.; Isacoff, E. Y.; Groves, J. T. Neuronal synapse interaction reconstituted between live cells and supported lipid bilayers. *Nat. Chem. Biol.* **2005**, *1* (5), 283–289.
(18) Parthasarathy, R.; Groves, J. T. Protein patterns at lipid bilayer junctions. *Proc. Natl. Acad. Sci. U.S.A.* **2004**, *101* (35), 12798–12803.
(19) Lee, K. H.; Dinner, A. R.; Tu, C.; Campi, G.; Raychaudhuri, S.; Varma, R.; Sims, T. N.; Burack, W. R.; Wu, H.; Kanagawa, O.; Markiewicz, M.; Allen, P. M.; Dustin, M. L.; Chakraborty, A. K.; Shaw, A. S. The immunological synapse balances T cell receptor signaling and degradation. *Science* **2003**, *302* (5648), 1218–1222.
(20) Tanaka, M.; Sackmann, E. Polymer-supported membranes as models of the cell surface. *Nature* **2005**, *437* (7059), 656–663.
(21) Cho, N. J.; Cheong, K. H.; Lee, C.; Frank, C. W.; Glenn, J. S. Binding dynamics of hepatitis C virus' NS5A amphipathic peptide to cell and model membranes. *J. Virol.* **2007**, *81* (12), 6682–9.
(22) Perez, T. D.; Nelson, W. J.; Boxer, S. G.; Kam, L. E-cadherin tethered to micropatterned supported lipid bilayers as a model for cell adhesion. *Langmuir* **2005**, *21* (25), 11963–11968.
(23) Svedhem, S.; Dahlborg, D.; Ekeroth, J.; Kelly, J.; Hook, F.; Gold, J. In situ peptide-modified supported lipid bilayers for controlled cell attachment. *Langmuir* **2003**, *19* (17), 6730–6736.

(24) Salafsky, J.; Groves, J. T.; Boxer, S. G. Architecture and function of membrane proteins in planar supported bilayers: A study with photosynthetic reaction centers. *Biochemistry* **1996**, *35* (47), 14773–14781.

(25) Ochsenhirt, S. E.; Kokkoli, E.; McCarthy, J. B.; Tirrell, M. Effect of RGD secondary structure and the synergy site PHSRN on cell adhesion, spreading and specific integrin engagement. *Biomaterials* **2006**, *27* (20), 3863–3874.

(26) Biesalski, M. A.; Knaebel, A.; Tu, R.; Tirrell, M. Cell adhesion on a polymerized peptide-amphiphile monolayer. *Biomaterials* **2006**, *27* (8), 1259–1269.

(27) Dillow, A. K.; Ochsenhirt, S. E.; McCarthy, J. B.; Fields, G. B.; Tirrell, M. Adhesion of alpha(5)beta(1) receptors to biomimetic substrates constructed from peptide amphiphiles. *Biomaterials* **2001**, *22* (12), 1493–1505.

(28) Pakalns, T.; Haverstick, K. L.; Fields, G. B.; McCarthy, J. B.; Mooradian, D. L.; Tirrell, M. Cellular recognition of synthetic peptide amphiphiles in self-assembled monolayer films. *Biomaterials* **1999**, *20* (23−24), 2265–2279.

(29) Zhang, F.; Shi, Z. L.; Chua, P. H.; Kang, E. T.; Neoh, K. G. Functionalization of titanium surfaces via controlled living radical polymerization: from antibacterial surface to surface for osteoblast adhesion. *Ind. Eng. Chem. Res.* **2007**, *46* (26), 9077–9086.

(30) Kadler, K. E.; Hill, A.; Canty-Laird, E. G. Collagen fibrillogenesis: fibronectin, integrins, and minor collagens as organizers and nucleators. *Curr. Opin. Cell Biol.* **2008**, *20* (5), 495−501.

(31) Buttafoco, L.; Engbers-Buijtenhuijs, P.; Poot, A. A.; Dijkstra, P. J.; Daamen, W. F.; van Kuppevelt, T. H.; Vermes, I.; Feijen, J. First steps towards tissue engineering of small-diameter blood vessels: preparation of flat scaffolds of collagen and elastin by means of freeze drying. *J. Biomed. Mater. Res.* **2006**, *77B* (2), 357–368.

(32) Wissink, M. J. B.; Beernink, R.; Pieper, J. S.; Poot, A. A.; Engbers, G. H. M.; Beugeling, T.; van Aken, W. G.; Feijen, J. Immobilization of heparin to EDC/NHS-crosslinked collagen. Characterization and in vitro evaluation. *Biomaterials* **2001**, *22* (2), 151–163.

(33) Angele, P.; Abke, J.; Kujat, R.; Faltermeier, H.; Schumann, D.; Nerlich, M.; Kinner, B.; Englert, C.; Ruszczak, Z.; Mehrl, R.; Mueller, R. Influence of different collagen species on physico-chemical properties of crosslinked collagen matrices. *Biomaterials* **2004**, *25* (14), 2831–2841.

(34) Nam, K.; Kimura, T.; Kishida, A. Preparation and characterization of cross-linked collagen-phospholipid polymer hybrid gels. *Biomaterials* **2007**, *28* (1), 1–8.

(35) Staros, J. V.; Wright, R. W.; Swingle, D. M. Enhancement by *N*-hydroxysulfosuccinimide of water-soluble carbodiimide-mediated coupling reactions. *Anal. Biochem.* **1986**, *156* (1), 220–222.

(36) Keller, C. A.; Kasemo, B. Surface specific kinetics of lipid vesicle adsorption measured with a quartz crystal microbalance. *Biophys. J.* **1998**, *75* (3), 1397–1402.

(37) Keller, C. A.; Glasmastar, K.; Zhdanov, V. P.; Kasemo, B. Formation of supported membranes from vesicles. *Phys. Rev. Lett.* **2000**, *84* (23), 5443–6.

(38) Cho, N. J.; Kanazawa, K. K.; Glenn, J. S.; Frank, C. W. Employing two different quartz crystal microbalance models to study changes in viscoelastic behavior upon transformation of lipid vesicles to a bilayer on a gold surface. *Anal. Chem.* **2007**, *79*, 7027–7035.

(39) Domack, A.; Prucker, O.; R?e, J. g.; Johannsmann, D. Swelling of a polymer brush probed with a quartz crystal resonator. *Phys. Rev. E* **1997**, *56* (1), 680.

(40) Voinova, M. V.; Rodahl, M.; Jonson, M.; Kasemo, B. Viscoelastic acoustic response of layered polymer films at fluid-solid interfaces: Continuum mechanics approach. *Phys. Scr.* **1999**, *59* (5), 391–396.

(41) Graneli, A.; Edvardsson, M.; Hook, F. DNA-based formation of a supported, three-dimensional lipid vesicle matrix probed by QCM-D and SPR. *ChemPhysChem* **2004**, *5* (5), 729–733.

(42) Axelrod, D.; Koppel, D. E.; Schlessinger, J.; Elson, E.; Webb, W. W. Mobility measurement by analysis of fluorescence photobleaching recovery kinetics. *Biophys. J.* **1976**, *16* (9), 1055–1069.

(43) Larsen, M.; Artym, V. V.; Green, J. A.; Yamada, K. M. The matrix reorganized: extracellular matrix remodeling and integrin signaling. *Curr. Opin. Cell Biol.* **2006**, *18* (5), 463–71.

(44) Brown, J. C.; Golbik, R.; Mann, K.; Timpl, R. Structure and stability of the triple-helical domains of human collagen XIV. *Matrix Biol.* **1994**, *14* (4), 287–95.

(45) Cho, N. J.; Cho, S. J.; Hardesty, J. O.; Glenn, J. S.; Frank, C. W. Creation of lipid partitions by deposition of amphipathic viral peptides. *Langmuir* **2007**, *23* (21), 10855–10863.

(46) Cho, N. J.; Cho, S. J.; Cheong, K. H.; Glenn, J. S.; Frank, C. W. Employing an amphipathic viral peptide to create a lipid bilayer on Au and TiO_2. *J. Am. Chem. Soc.* **2007**, *129* (33), 10050–1.

(47) Reimhult, E.; Hook, F.; Kasemo, B. Vesicle adsorption on SiO_2 and TiO_2: Dependence on vesicle size. *J. Chem. Phys.* **2002**, *117* (16), 7401–7404.

(48) Larsson, C.; Bramfeldt, H.; Wingren, C.; Borrebaeck, C.; Hook, F. Gravimetric antigen detection utilizing antibody-modified lipid bilayers. *Anal. Biochem.* **2005**, *345* (1), 72–80.

(49) Glasmastar, K.; Larsson, C.; Hook, F.; Kasemo, B. Protein adsorption on supported phospholipid bilayers. *J. Colloid Interface Sci.* **2002**, *246* (1), 40–47.

(50) Singer, S. J.; Nicolson, G. L. The fluid mosaic model of the structure of cell membranes. *Science* **1972**, *175* (23), 720–31.

(51) Fahey, P. F.; Koppel, D. E.; Barak, L. S.; Wolf, D. E.; Elson, E. L.; Webb, W. W. Lateral diffusion in planar lipid bilayers. *Science* **1977**, *195* (4275), 305–6.

(52) Zhang, L. F.; Granick, S. Slaved diffusion in phospholipid bilayers. *Proc. Natl. Acad. Sci. U.S.A.* **2005**, *102* (26), 9118–9121.

(53) Disatnik, M. H.; Rando, T. A. Integrin-mediated muscle cell spreading. The role of protein kinase c in outside-in and inside-out signaling and evidence of integrin cross-talk. *J. Biol. Chem.* **1999**, *274* (45), 32486–92.

(54) Andersson, A. S.; Glasmastar, K.; Sutherland, D.; Lidberg, U.; Kasemo, B. Cell adhesion on supported lipid bilayers. *J. Biomed. Mater. Res.* **2003**, *64A* (4), 622–629.

(55) Zhdanov, V. P.; Kasemo, B. Van der Waals interaction during protein adsorption on a solid covered by a thin film. *Langmuir* **2001**, *17* (18), 5407–5409.

(56) Cukierman, E.; Pankov, R.; Yamada, K. M. Cell interactions with three-dimensional matrices. *Curr. Opin. Cell Biol.* **2002**, *14* (5), 633–9.

(57) Reimhult, E.; Hook, F.; Kasemo, B. Intact vesicle adsorption and supported biomembrane formation from vesicles in solution: influence of surface chemistry, vesicle size, temperature, and osmotic pressure. *Langmuir* **2003**, *19*, 1681–1691.

(58) Gurdak, E.; Dupont-Gillain, C. C.; Booth, J.; Roberts, C. J.; Rouxhet, P. G. Resolution of the vertical and horizontal heterogeneity of adsorbed collagen layers by combination of QCM-D and AFM. *Langmuir* **2005**, *21* (23), 10684–10692.

(59) De Cupere, V. M.; Van Wetter, J.; Rouxhet, P. G. Nanoscale organization of collagen and mixed collagen-pluronic adsorbed layers. *Langmuir* **2003**, *19* (17), 6957–6967.

(60) Denis, F. A.; Hanarp, P.; Sutherland, D. S.; Gold, J.; Mustin, C.; Rouxhet, P. G.; Dufrene, Y. F. Protein adsorption on model surfaces with controlled nanotopography and chemistry. *Langmuir* **2002**, *18* (3), 819–828.

(61) Yoshina-Ishii, C.; Miller, G. P.; Kraft, M. L.; Kool, E. T.; Boxer, S. G. General method for modification of liposomes for encoded assembly on supported bilayers. *J. Am. Chem. Soc.* **2005**, *127* (5), 1356–1357.

(62) Gilmanshin, R.; Creutz, C. E.; Tamm, L. K. Annexin-Iv reduces the rate of lateral lipid diffusion and changes the fluid-phase structure of the lipid bilayer when it binds to negatively charged membranes in the presence of calcium. *Biochemistry* **1994**, *33* (27), 8225–8232.

(63) Cezanne, L.; Lopez, A.; Loste, F.; Parnaud, G.; Saurel, O.; Demange, P.; Tocanne, J. F. Organization and dynamics of the proteolipid complexes formed by annexin V and lipids in planar supported lipid bilayers. *Biochemistry* **1999**, *38* (9), 2779–2786.

(64) Yamazaki, V.; Sirenko, O.; Schafer, R. J.; Groves, J. T. Lipid mobility and molecular binding in fluid lipid membranes. *J. Am. Chem. Soc.* **2005**, *127* (9), 2826–2827.

(65) Naumann, C. A.; Prucker, O.; Lehmann, T.; Ruhe, J.; Knoll, W.; Frank, C. W. The polymer-supported phospholipid bilayer: Tethering as a new approach to substrate-membrane stabilization. *Biomacromolecules* **2002**, *3* (1), 27–35.

(66) Zhang, L. F.; Granick, S. Interleaflet diffusion coupling when polymer adsorbs onto one sole leaflet of a supported phospholipid bilayer. *Macromolecules* **2007**, *40* (5), 1366–1368.

(67) Tournier, J. F.; Lopez, A.; Tocanne, J. F. Effect of cell substratum on lateral mobility of lipids in the plasma-membrane of vascular endothelial-cells. *Exp. Cell Res.* **1989**, *181* (1), 105–115.

BM901445R